

Numerical Simulations of the Flows Past Rotating Geometries

Jakub SIMON
jakub.simon@o2.pl

Witold STANKIEWICZ

*Poznan University of Technology, Institute of Applied Mechanics, ul. Jana Pawła II 24,
60-965 Poznań, Poland, witold.stankiewicz@put.poznan.pl*

Abstract

In the present paper the numerical approach for the modeling of the flow past rotating geometries is presented. Practical methods for two cases are described: the one where whole domain is moving with uniform angular velocity, where the rotation might be included in the governing equations only (in the terms related to Coriolis and centrifugal forces), and the one where part of the domain is rotating, whereas another one is stationary. The second case is illustrated by examples describing the steady and transient flow around a rotating propeller and by a centrifugal pump. Simulations are performed using OpenFOAM CFD solver, with the models covering flow rotation: MRF (multiple reference frame) and AMI (arbitrary mesh interface).

Keywords: CFD, rotating geometry, OpenFOAM, Fluid-Structure Interaction (FSI), propeller, pump

1. Introduction

Rotating elements occur in many flows of fundamental engineering importance. Fluid flow machinery are devices in which the fluid flows continuously, and its energy is transferred from or to the working medium as a result of dynamic interaction with stationary and rotating parts of the machine. Fluid flow machines can be divided into the rotor ones, which include compressors, pumps, fans, propellers and various turbines, as well as jet machines, which include, among others, injectors and jet engines [1,2]. These machines play a key role in the energy industry, including the use of renewable energy sources, are used in floating and flying vehicles, from drones to airliners and large cruise ships.

Modeling the flow with rotating geometry is not straightforward and often requires interpolation between the stationary and rotating areas, as well as the use of additional terms in the governing equations. It might include the interactions between the fluid and the structure as well, leading to computation of flow-induced vibrations and analysis of phenomena like flutter and buffeting, simulation of flapping flight or analysis of a flow past flexible and deforming/morphing bodies.

In this paper, two test cases are presented to demonstrate OpenFOAM flow analysis around rotating geometries.

2. Mathematical formulation and methodology of computations

Fluid flow might be modeled using Navier-Stokes equations in the form:

$$\begin{cases} \frac{\partial(\rho \mathbf{u})}{\partial t} + \nabla \cdot (\rho \mathbf{u} \otimes \mathbf{u}) = -\nabla p + \nabla \cdot (\mu \nabla \mathbf{u}) \\ \nabla \cdot \mathbf{u} = 0 \end{cases} \quad (1)$$

where: \mathbf{u} is (absolute) velocity of the flow, p is pressure, ρ is density and μ is viscosity. The motion of the geometry can be taken into account in several ways.

When the whole domain moves with common velocity, this motion might be included as additional terms in the governing equation, and the mesh nodes do not actually move. In the case of single, rotating domain, these additional terms correspond to Coriolis ($2\rho\boldsymbol{\Omega} \times \mathbf{u}_R$) and centrifugal ($\rho\boldsymbol{\Omega} \times (\boldsymbol{\Omega} \times \mathbf{r})$) forces, and the resulting Navier-Stokes equations in rotating domain might be written as follows [3]:

$$\begin{cases} \frac{\partial(\rho \mathbf{u}_R)}{\partial t} + (\rho \mathbf{u}_R \cdot \nabla) \mathbf{u}_R + 2\rho\boldsymbol{\Omega} \times \mathbf{u}_R + \rho\boldsymbol{\Omega} \times (\boldsymbol{\Omega} \times \mathbf{r}) = -\nabla p + \nabla \cdot (\mu \nabla \mathbf{u}_R) \\ \nabla \cdot \mathbf{u}_R = 0 \end{cases} \quad (2)$$

where: $\boldsymbol{\Omega}$ means rotational velocity, \mathbf{r} is the radius from the axis of rotation, and \mathbf{u}_R is relative velocity defined as:

$$\mathbf{u}_R = \mathbf{u} - \boldsymbol{\Omega} \times \mathbf{r} \quad (3)$$

In OpenFOAM CFD software [4], this case is referred as SRF (single reference frame) model [3,5].

If not the entire domain is to be rotated, Multiple Reference Frame (MRF) approach is available [3]. In MRF model, we assume that the movement of one (or more) parts of the geometry is rotational, while some other are stationary.

There are separate governing equations for the stationary and the rotating zones, separated from the computational mesh. For the rotating one, we include relative velocity \mathbf{u}_R as well as absolute velocity \mathbf{u} , and the equations might be derived by the rearrangement of the equations for SRF model [5] (4):

$$\begin{cases} \frac{\partial(\rho \mathbf{u}_R)}{\partial t} + \nabla \cdot (\rho \mathbf{u}_R \otimes \mathbf{u}) + \rho\boldsymbol{\Omega} \times \mathbf{u} = -\nabla p + \nabla \cdot (\mu \nabla \mathbf{u}) \\ \nabla \cdot \mathbf{u}_R = 0 \end{cases} \quad (4)$$

For the stationary zone, default Navier-Stokes equations (1) are used. In all these zones, as in the case of SRF, mesh nodes do not move.

Another case is the flow around a geometry that (or part of it) oscillates at a limited (small) amplitude. In such a situation, Arbitrary Lagrangian-Eulerian (ALE) formulation [6, 7] might be used:

$$\begin{cases} \frac{\partial(\rho \mathbf{u})}{\partial t} + \nabla \cdot (\rho \mathbf{u} \otimes (\mathbf{u} - \mathbf{u}_{grid})) = -\nabla p + \nabla \cdot (\mu \nabla \mathbf{u}) \\ \nabla \cdot \mathbf{u} = 0 \end{cases} \quad (5)$$

Here, \mathbf{u}_{grid} represents velocity of the moving (deforming) mesh. The mesh motion, related to the oscillation of the geometry, might be pre-defined, or a result of the structure deformation forced by aerodynamic loads, computed in FSI (Fluid-Structure Interactions), or aeroelastic, simulation. In such a simulation, coupling between CFD and structural FEM codes is done by interpolation of variables like aerodynamic forces and translations between two codes, possibly on non-conforming meshes.

This approach might be applied to flutter analysis, simulation of flapping flight or flow past flexible airfoil (Fig. 1) [8], as well as in many other cases.

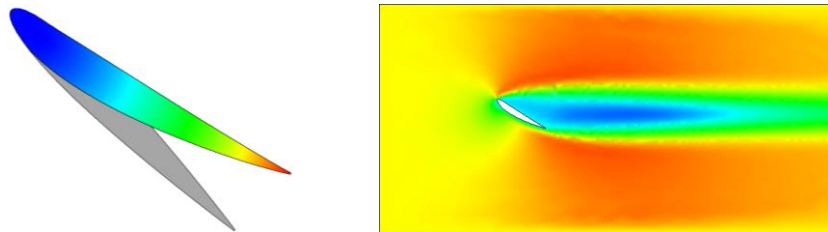


Figure 1. Static deformation of the structure (left) and steady velocity field (right) for incompressible flow past NACA-0012 airfoil, at $Re=100$ and angle of attack $\alpha = 45^\circ$ [8].

Use of this approach is limited by the amplitude of mesh motion – its deformation results in the change of mesh elements' shape, which leads to deterioration of mesh quality and eventually – to the loss of simulation's convergence.

Finally, the case where part of the domain (geometry) is moving with large displacements is considered. In such a case, both previously mentioned approaches are not applicable. The solution is to divide the computational domain into parts: stationary and moving (rotating) one. This approach, depending on the software developer and technical details, is called overlapping mesh or Chimera technique [9, 10].

Arbitrary motion of the moving domain is included in the governing equations using ALE-like approach, by additional convective term related to mesh velocity. Overlapping regions of the two (or more) meshes are used to interpolate and reconcile the values of variables in two domains analyzed simultaneously (Fig. 2).

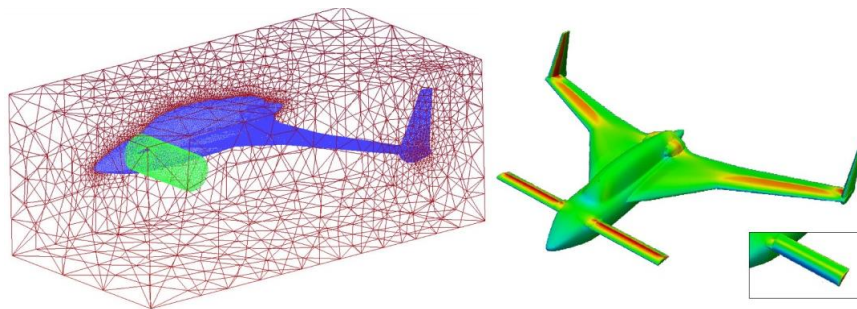


Figure 2. Meshes for static (rectangular) and rotating (cylindrical) Chimera domains (left) and the results for a flow past an aircraft at canard's angles of attack: $5^\circ / -20^\circ$ [9].

In OpenFOAM, similar approach called Arbitrary Meshing Interface (AMI) [3], enabling simulation across disconnected, adjacent, mesh domains, whose elements partially overlap each other, is available.

In this approach, additional, auxiliary AMI zones (patches) are used to set the connection between nodes (and elements) from stationary and rotating zones, using their coordinates for current time step.

3. Steady flow past a propeller

The first test case chosen for the analyses of the flow past rotating geometries is a propeller dedicated to a small aircraft, based on the model available at [11]. Its main dimensions, including the pitch, are depicted on Fig. 3.

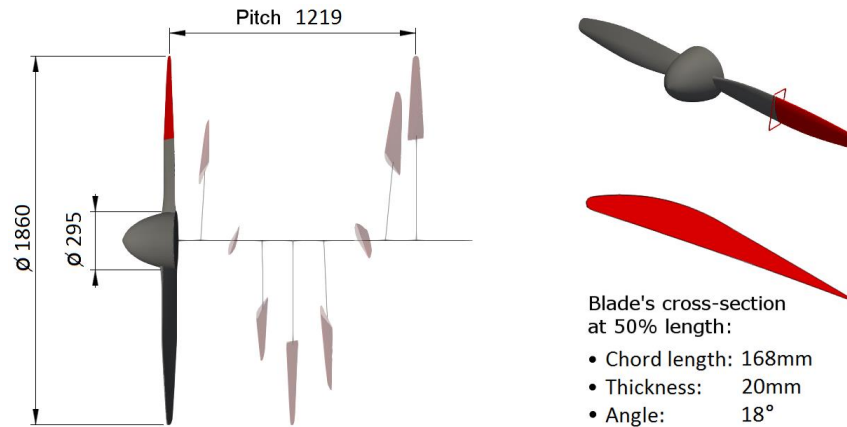


Figure 3. Basic dimensions of the propeller model.

The computational domain (Fig.4, left) has been divided into two zones: stationary (rectangular) and rotating one (cylindrical, with diameter of 2000 mm and height of 450 mm), with additional AMI interface made of triangular elements lying between them. The generated computational mesh, generated using *snappyHexMesh* tool, consists in 3.3 million elements (Fig. 4, right).

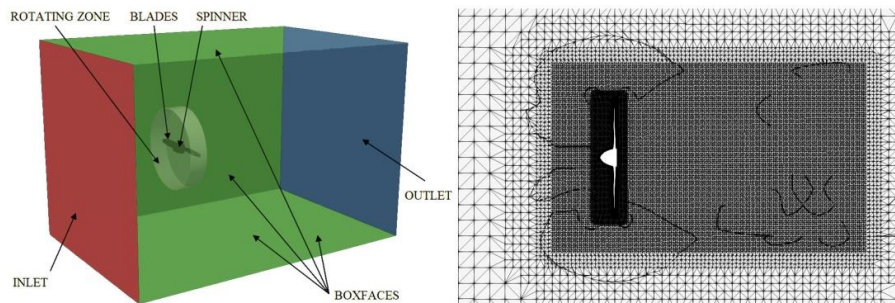


Figure 4. Computational domain (left) and the mesh (right) for the flow past a propeller

The steady flow has been simulated using *simpleFoam* solver, with $k-\omega$ SST turbulence model [12]. Kinematic viscosity has been set to $1.81 \cdot 10^{-5} \text{ m}^2/\text{s}$. Boundary conditions have been set as follows: on inlet, the velocity was constant (30 m/s), on outlet, *inletOutlet* boundary condition has been chosen. It switches between *zeroGradient* when the fluid flows out of the domain, and *fixedValue*, when the fluid is

flowing into the domain. Rotation of the propeller (within cylindrical zone) has been set to values 209 rad/s (2000 RPM) and 419 rad/s (4000 RPM). On the rest of domain's external faces, slip condition has been set. The results of the flow for these two angular velocities of the propeller, are shown in Fig. 5.

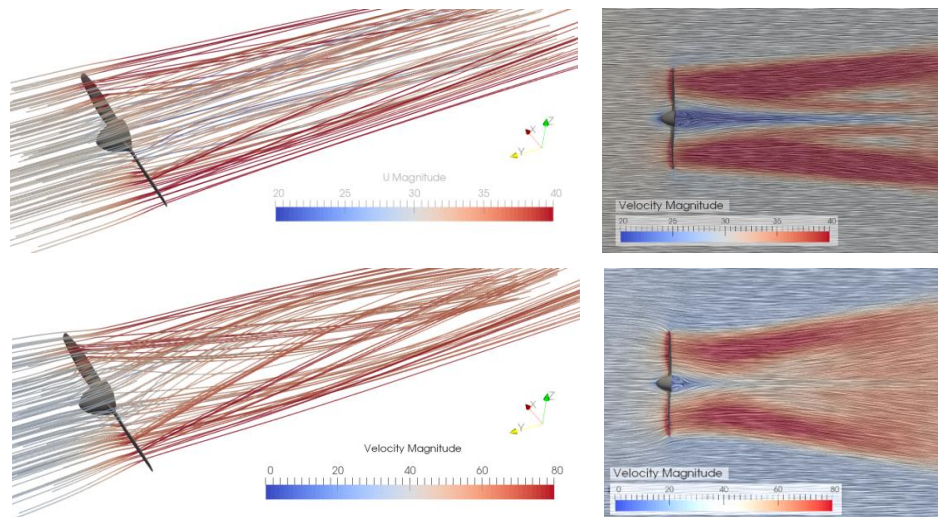


Figure 5. Streamlines (left) and surface LIC (right) visualizations for the flow past the propeller rotating at 2000 RPM (top) and 4000 RPM (bottom).

As expected, higher angular velocity generates more whirled flow behind the propeller. The velocity magnitude increases for more revolutions per minute. The computed thrust, generated by the propeller, is 788N for angular velocity equal to 2000 RPM and 5595N for 4000 RPM. That means, not taking into account the drag generated by whole aircraft, that the considered flight speed will tend to increase, especially at higher rotational velocity of the propeller.

4. Transient flow past a centrifugal pump

The second test case illustrating flow simulations in rotating geometries is centrifugal pump model created by R. Maleki [13]. The geometry has been divided into four parts: pump's body, rotor blades, base of the rotor blades and rotating zone (Fig. 6, left). Again, the computational mesh has been generated using *snappyHexMesh* tool. It consists in one million elements (Fig.6, right).

The inlet boundary conditions have been defined as constant volume flow rate, and the *inletOutlet* condition has been used for the outflow. On the walls of the body, flow velocity is zero. Angular velocity of the blades is 157 rad/s, what is equivalent to 1500 revolutions per minute. Kinematic viscosity of the fluid has been set to $1.006 \cdot 10^{-6} \text{ m}^2/\text{s}$, corresponding to water at 20 °C.

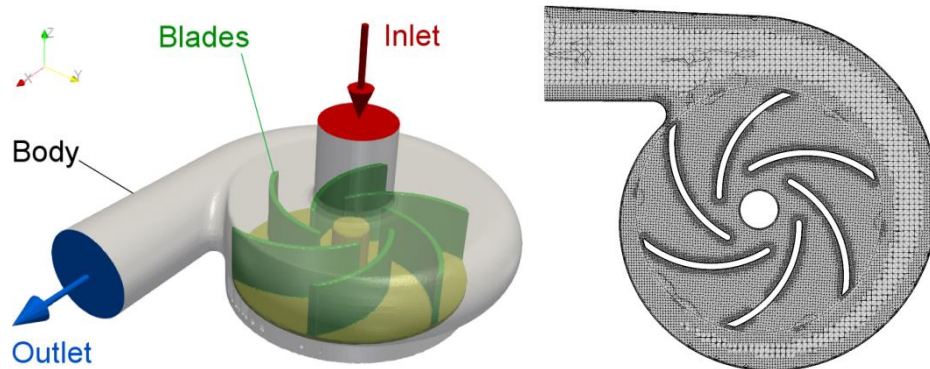


Figure 6. Geometry of centrifugal pump (left) [13], and the generated computational mesh (right).

The flow has been analyzed using two approaches: steady RANS equations with $k-\omega$ SST turbulence model and MRF model for rotating zone, where the solution is time-averaged [14], and Detached Eddy Simulation (DES) model with $k\Omega$ SSTDES subgrid turbulence model [15] and Arbitrary Meshing Interface. For transient simulation, *pimpleFoam* solver has been used, with time step $dt = 10^{-5}$ s.

The velocity magnitudes for steady solution (obtained with RANS and MRF model) and the instantaneous solution (obtained with DES and AMI) for $t = 0.24$ s, are compared in Fig. 7, on the plane normal to the rotation axis. Analyzing the velocity fields it can be concluded that both solutions are comparable, whereby the DES model, as expected, is characterized by more complex coherent structures.

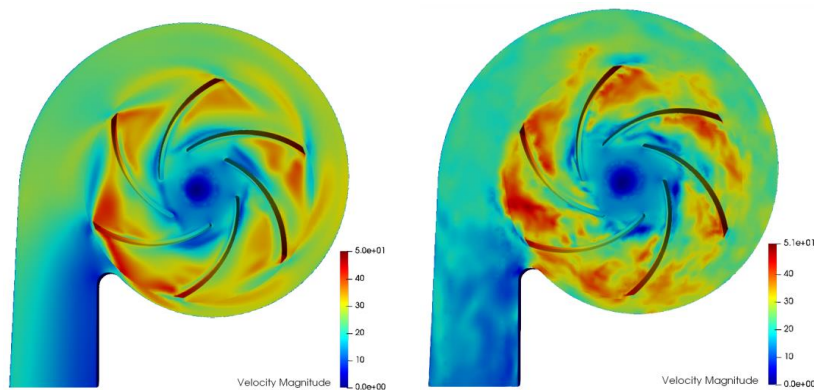


Figure 7. Time-averaged velocity magnitude for steady RANS simulation (left) and instantaneous solution at $t=0.24$ s for transient DES simulation (right).

For the DES transient solution, pressure field and the streamlines inside of the pump, are depicted in Fig. 8.

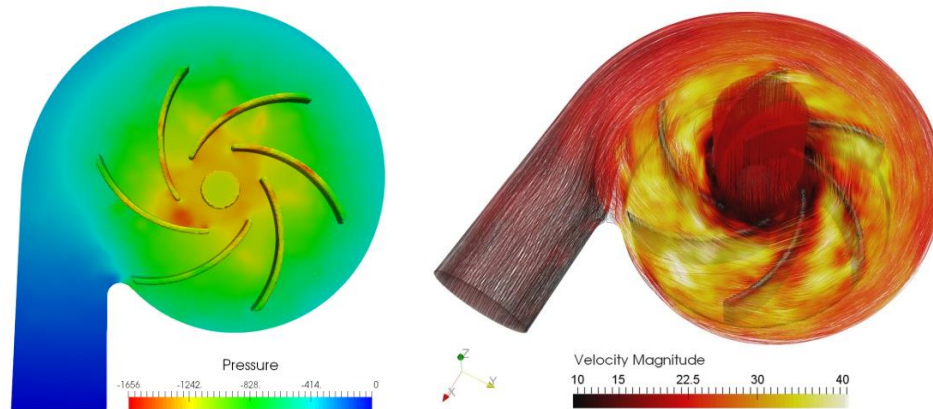


Figure 8. Instantaneous pressure field (left) and flow (right) inside the centrifugal pump.

It can be seen, that both velocities and pressures vary depending on the position of the blade inside the pump. This leads to a variation in the load on each blade throughout its rotation, which can lead to flow-induced vibration. This phenomena, although should be modeled and analyzed taking into account fluid-structure interactions.

5. Conclusions

This paper presents numerical techniques used to simulate flows, in which part of the domain rotates. These methods, illustrated on the examples of flows around the propeller and through the centrifugal pump, are of great importance in modern industry.

Discussed approaches might be used to evaluate new designs. The simulation results can be used to determine the thrust, moments, and in the case of pumps: pressure differences, which allows to determine their efficiency and head. In the case of presented pump, these values are $\eta = 0,77$ and $H = 117\text{m}$, respectively.

The data from CFD simulations can be used to determine the efficiency curve depending on the rotational speed and determine the most favorable operating parameters.

Coupling of the fluid flow simulation with the structural analysis might lead to estimation and further avoiding of flow-induced vibrations. The simulation results can also be used to compare different blade settings and different propeller and pump models.

Acknowledgments

This work was supported by grants of the Ministry of Science and Higher Education in Poland no 0612/SBAD/3567.

References

1. T. J. Chmielniak, *Maszyny przepływowe*. Wydawnictwo Politechniki Śląskiej, 1997.
2. T. Wright, *Fluid machinery. Performance, analysis and design*. CRC Press, 1999.
3. D. Wilhelm, *Rotating Flow Simulations with OpenFOAM*. International Journal of Aeronautical Science and Aerospace Research. S1:001 (2015) 1-7.
4. G. Holzinger, *OpenFOAM - a little user-manual. CD-Laboratory-Particulate Flow Modelling*, Johannes Kepler University. Linz, Austria, 2015.
5. F. Nozaki, *CFD for Rotating Machinery*. <https://www.slideshare.net/fumiyanozaki96/cfd-for-rotating-machinery-using-openfoam>
6. J. Donea, S. Giuliani, and J.P. Halleu, *An arbitrary Lagrangian-Eulerian finite element method for transient dynamic fluid-structure interactions*. Comput. Meths. Appl. Mech. Engrg. 33 (1982) 689–723.
7. W. Stankiewicz, M. Morzyński, R. Roszak, B.R. Noack, G. Tadmor, *Reduced order modelling of a flow around an airfoil with a changing angle of attack*. Archives of Mechanics 60:6 (2008) 509-526.
8. W. Stankiewicz, M. Morzyński, R. Roszak, *Numerical simulation of the flow past a flexible airfoil*. Proceedings of the International Conference on Innovative Technologies, Budapest (2013) 337-340.
9. P. Kwiek, *Implementation of the Chimera technique in the Edge flow program*. Master thesis, Poznan University of Technology, 2012 (in Polish).
10. R. Roszak, M. Morzyński, M. Nowak, W. Stankiewicz, H. Hausa, *Aeroelastic analysis for high-lift devices using chimera method*. Short papers of 20th Int. Conf. on Computer Methods in Mechanics (CMM-2013), Poznan (2013) 459-460.
11. <https://grabcad.com/library/small-airplane-propeller>.
12. F.R. Menter, M. Kuntz, and R. Langtry. *Ten years of industrial experience with the SST turbulence model*. Proceedings of the fourth international symposium on turbulence, heat and mass transfer, Antalya, Turkey (2003) 625–632.
13. <https://grabcad.com/library/centrifugal-pump-impeller-volute-casing-1>.
14. J. Simon, *Application of the MRF method and AMI algorithm in flow simulations with rotating geometry*. Master thesis, Poznan University of Technology, 2020 (in Polish).
15. M.S. Gritskevich, A.V. Garbaruk, J. Schuetze, F.R. Menter, *Development of DDES and IDDES Formulations for the k-omega Shear Stress Transport Model*. Flow, Turbulence and Combustion, 88:3 (2012) 431-449.